ACS Medicinal Chemistry Letters

Letter

pubs.acs.org/acsmedchemlett

Discovery of Mechanism-Based Inactivators for Human Pancreatic Carboxypeptidase A from a Focused Synthetic Library

Sebastián A. Testero,[†,§] Carla Granados,[‡] Daniel Fernández,[‡] Pablo Gallego,[‡] Giovanni Covaleda,[‡] David Reverter,[‡] Josep Vendrell,[‡] Francesc X. Avilés,[‡] Irantzu Pallarès,[*,‡] and Shahriar Mobashery[*,†]

[†]Department of Chemistry and Biochemistry, University of Notre Dame, Notre Dame, Indiana 46556, United States

[‡]Departament de Bioquímica i Biologia Molecular, Facultat de Biociències, and Institut de Biotecnologia i de Biomedicina, Universitat Autònoma de Barcelona, E-08193 Bellaterra, Spain

Supporting Information

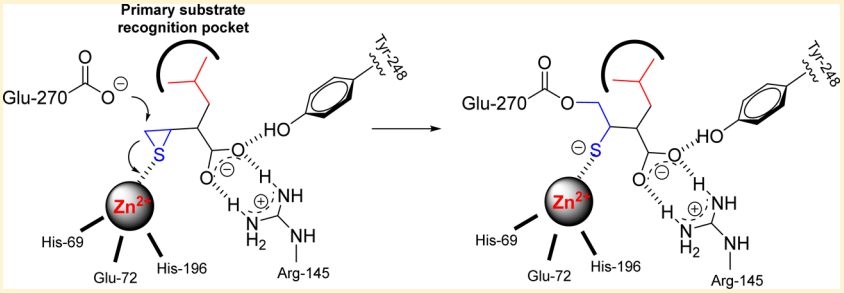

ABSTRACT: Metallocarboxypeptidases (MCPs) are involved in many biological processes such as fibrinolysis or inflammation, development, Alzheimer's disease, and various types of cancer. We describe the synthesis and kinetic characterization of a focused library of 22 thiirane- and oxirane-based potential mechanism-based inhibitors, which led to discovery of an inhibitor for the human pro-carboxypeptidase A1. Our structural analyses show that the thiirane-based small-molecule inhibitor penetrates the barrier of the pro-domain to bind within the active site. This binding leads to a chemical reaction that covalently modifies the catalytic Glu270. These results highlight the importance of combined structural, biophysical, and biochemical evaluation of inhibitors in design strategies for the development of spectroscopically nonsilent probes as effective beacons for *in vitro*, *in cellulo*, and/or *in vivo* localization in clinical and industrial applications.

KEYWORDS: *Carboxypeptidase A, mechanism-based inactivators, thiiranes, X-ray crystallography*

The human genome is reported to have about 600 proteases of which approximately 150 are believed to be zinc-dependent.[1] These can cleave within a stretch of a polypeptide (endopeptidases) or release amino acids from either termini of the polypeptides (exopeptidases). Metallocarboxypeptidases (MCPs) excise one amino acid at a time from the C-terminal end of the polypeptide substrates. These enzymes had been historically considered important for digestive functions, as exemplified by the now-classical examples of the bovine pancreatic carboxypeptidases A and B. This limited role for these enzymes has been refuted on the basis of the genomic information and biochemical discoveries in recent years.[2,3] Now, MCPs are subdivided into the A/B subfamily (M14A according to MEROPS), the N/E subfamily (M14B), the γ-D-glutamyl-*meso*-diaminopimelate peptidase I (M14C), and the complex cytosolic carboxypeptidases, CCPs (M14D).[4,5] These enzymes are currently known to be expressed in all tissues and likely have functions in maturation of neuropeptides, hormones, and cytokines, in blood fibrinolysis, in anaphylaxis, among others. A variety of MCPs have been linked to human diseases such as acute pancreatitis, type 2 diabetes, Alzheimer's disease, and various types of cancer.[6−11] Due to their proteolytic nature, MCP functions are strictly regulated by means of controlled secretion, compartmentalization, substrate specialization, or expression as inactive enzymes (zymogens), typically seen in the M14A subfamily.

Small-molecule inhibitors of various types have been developed to target MCPs specifically; among them, there has been considerable interest in irreversible mechanism-based enzyme inhibitors.[12−14] These compounds are inert species that bind to their respective target enzymes based on inherent affinity designed into the molecular scaffolding. Upon binding, a reaction leading to covalent inhibition irreversibly modifies the enzyme active site limiting the opportunity for unwanted cross-reactions. The prolonged longevity of the covalently inhibited species confers to these compounds' desirable attributes as pharmaceuticals, imaging reagents, mechanistic tools, and diagnostic agents[15,16]

A few strategies for mechanism-based inhibition of zinc proteases have been described in the literature.[13,17−19] Two are

Received: August 21, 2017
Accepted: September 22, 2017
Published: September 22, 2017

DOI: 10.1021/acsmedchemlett.7b00346
ACS Med. Chem. Lett. 2017, 8, 1122−1127

based on the chemistries of oxiranes and thiiranes, whose structural scaffolds dock into the S1′ specificity pocket, typically through a single amino acid side chain. The terminal carboxylate, as a recognition element for the MCPs, is matched by a positively charged amino acid on the part of the enzyme. These interactions bring the heteroatoms in the thiirane or oxirane into the coordination sphere of the zinc ion, predisposing the compounds for covalent modification by an active-site nucleophile, typically the catalytic glutamate of MCPs (Scheme 1).[20,21] The thiirane-based mechanism-based

Scheme 1. Recognition of a Polypeptide Substrate within the MCPs Active Site (Top Panel; Boxed), Mimicked by That of a Thiirane- or Oxirane-Based Inhibitors[a]

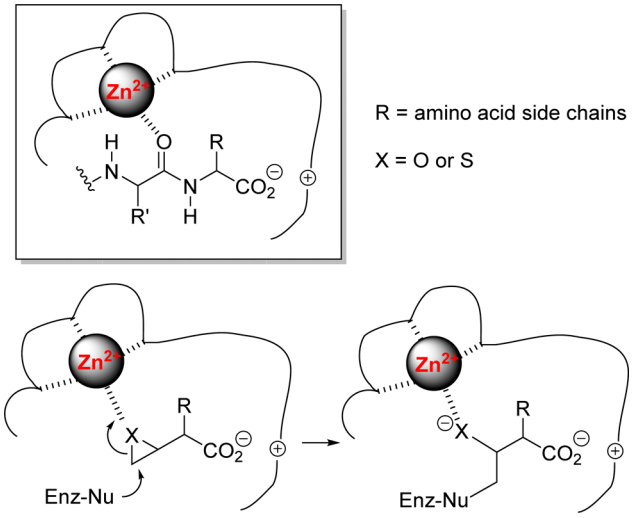

[a]The metal-ion coordination chemistry is necessary for the onset of covalent modification.

inhibitors may also lead to a reaction that generates a thiolate within the active site, which results in tight-binding inhibition of the target enzyme.[14,19]

Inspired by the known inhibitors BEBA and BTBA, we report herein the preparation of a focused library of 22 thiirane- and oxirane-based potential MCP irreversible inhibitors (Figure 1). This library was first screened for inhibition of the activated bovine caboxypeptidases A (bCPA) and B (bCPB). Then, promising inhibitors were screened against the human pancreatic CPA1 proenzyme (hproCPA1). In hproCPA1, the prodomain is loosely capping the active site of the enzyme, and small molecules can gain access to the active site. We identified one compound, the racemic mixture of *trans*-4-methyl-2-(thiiran-2-yl)pentanoic acid (**11**), as a covalent modifier of the enzyme. We also report the X-ray structure of the hproCPA1-inhibitor **11** complex at 1.8 Å resolution, which represents the first for a covalently inhibited zymogen. This study provides for the first time structural evidence on the capacity of low-molecular-weight compounds to diffuse into the active site of a zymogen, as previously inferred from the intrinsic activity of pro-CPs.[22] It is important to note that the inhibitor was prepared as a racemate, but only one enantiomer was seen within the active site (discussed below).

Scheme 2 shows the general synthetic method for the preparation of the library. The synthesis of oxiranes and thiiranes began with alkylation of vinyl acetic acid with eight different alkyl halides in moderate to good yields.[23] The

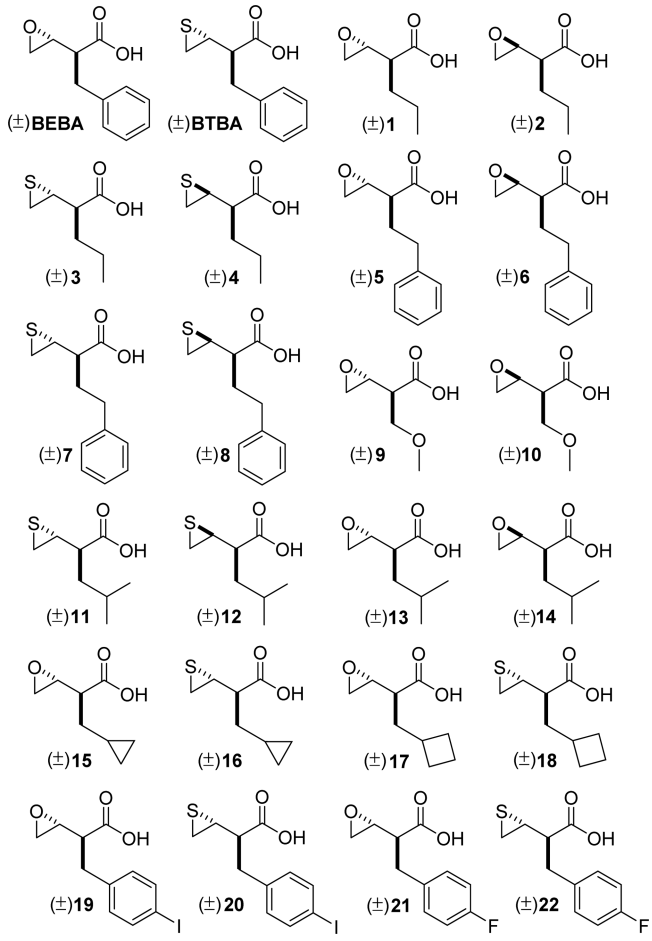

Figure 1. Library of synthetic oxiranes and thiiranes. Each compound was synthesized as a racemic mixture.

Scheme 2. General Synthetic Scheme for the Preparation of Compound Libraries

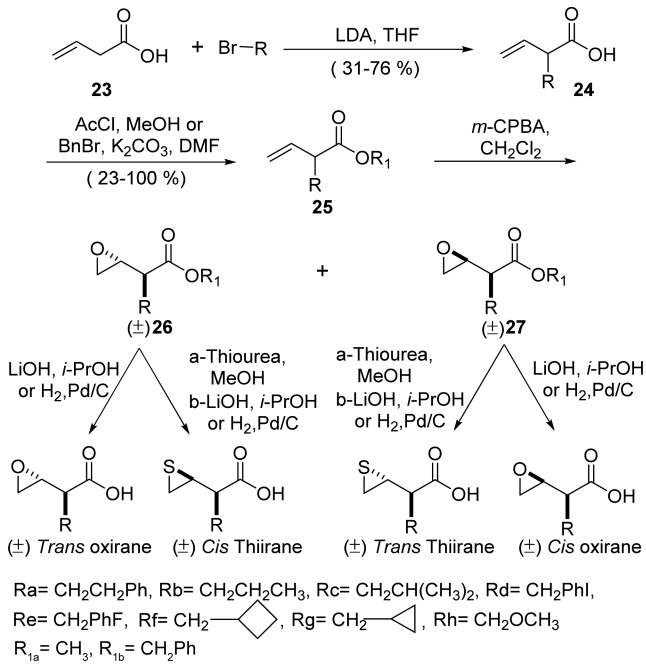

DOI: 10.1021/acsmedchemlett.7b00346
ACS Med. Chem. Lett. 2017, 8, 1122−1127

racemic α-substituted β,γ-unsaturated carboxylic acids were esterified as methyl or benzyl ester by standard methodologies. Epoxidation of the substituted 2-vinyl propanoate esters **25** provided the separable mixture of *trans* (**26**; major) and *cis* (**27**; minor) epoxides.[24] With the derivatives **26** in hand, the *trans* oxiranes **1**, **5**, **9**, **13**, **15**, **17**, **19**, and **21** were obtained by treatment with lithium hydroxide or hydrogenolysis over Pd/C. However, treatment of derivatives **26** with thiourea, followed by hydrolysis afforded the corresponding *cis* thiiranes **4**, **8**, and **12**. It is worth noting that conversion of the epoxide to the corresponding thiirane occurs with inversion of configuration.[21] Similarly, syntheses of the *cis* oxiranes **2**, **6**, **10**, and **14** and the *trans* thiiranes **3**, **7**, **11**, **16**, **18**, **20**, and **22** were accomplished from the derivatives **27** by the same strategy. All compounds were prepared in racemic forms. Cognizant of the fact that only the *trans* oxiranes and thiiranes have been shown to be active against carboxypeptidases,[25] we synthesized all the *trans* analogues of these two families. Regardless, we also synthesized some *cis* derivatives (from compounds **26** and **27**) to test their activity and to confirm that they are less active than the *trans* ones.

The library was first screened against the commercially available bovine CPA and CPB (see Supporting Information, Table S1). The two aforementioned oxirane and thiirane inhibitors for bCPA, compounds designated as BEBA and BTBA,[21] were also included as positive controls. The observation of time dependence for inhibition by mechanism-based inhibitors is a diagnostic criterion. As such, the screening comprised a short (2 min) and a long (3 h) preincubation of the compounds with the enzyme prior to activity assays. This criterion identified 15 compounds that inhibited bCPA activity (of which, incidentally, none inhibited bCPB; data not shown). Based on the IC_{50} values that we evaluated (Table S1), six compounds of the 15 (**3**, **11**, **19**, **20**, **21** and **22**) were selected for further analysis with the human pancreatic CPA (hCPA1; Table S2).

The inactivation reaction of hCPA1 by the above-mentioned inhibitors could be represented by eq 1 in the Supporting Information. The values of k_{obs} were calculated from plots of $\ln(v/v_o)$ vs incubation time (see Supporting Information). The parameters K_i^{app} and k_{inact} for the process were obtained from the plot of k_{obs} vs $[I]$ in a double-reciprocal fashion.[26] The kinetic parameters for hCPA1 inactivation for all the selected inhibitors are included in Table S2. All efforts in crystallization of the activated human CPA1 (lacking the pro domain) in complex with the selected inhibitors were not successful. Hence, we focused our attention on the crystallization of human pro-CPA1 (the zymogen).

All six compounds were tried in crystallographic characterization with the human enzyme; only inhibitor **11** produced results for a complex. The crystals diffracted to 1.8 Å resolution, and the crystallographic and refinement statistics details are presented in Table 1. The structure reported herein represents the first crystal structure of any zymogen of the carboxypeptidase family in complex with a small-molecule mechanism-based inhibitor.

Figure 2A shows a stereoview of the hpro-CPA-inhibitor **11** complex. The pro-domain, albeit capping the entrance to the active site, displays a flexibility that allows for a measurable intrinsic activity due to the diffusion of small-molecular-weight substrates.[27] The presence of contiguous electron density clearly indicated that the atoms constituting the thiirane moiety of the inhibitor were covalently attached to the side chain of

Table 1. Data Collection and Refinement Statistics

data collection	inhibitor: hproCPA1
space group	$P12_11$
cell dimensions	
a, *b*, *c* (Å)	53.90, 52.54, 133.97
α, β, γ (deg)	90.00, 95.00, 90.00
resolution[a] (Å)	44.50−1.77 (1.86−1.77)
R_{merge}[b]	0.07 (0.13)
$I/\sigma I$	10.2 (4.2)
completeness (%)	94.1 (66.0)
redundancy	3.1 (2.2)
refinement	
resolution (Å)	43.68−1.80
no. of reflections	63,800
R_{work}/R_{free}[c]	15.45/21.18
no. of atoms	6751
protein	6283
water	443
r.m.s. deviations	
bond lengths (Å)	0.022
bond angles (deg)	1.852
PDB code	5OM9

[a]Statistic for highest resolution shell is shown in parentheses. [b]$R_{merge} = \Sigma||I_i - \langle I\rangle|/\Sigma I_i$, where I_i is the *i*th measurement of the intensity of an individual reflection or its symmetry-equivalent reflections and $\langle I\rangle$ is the average intensity of that reflection and its symmetry-equivalent reflections. [c]$R_{work} = \Sigma||F_o| - |F_c||/\Sigma|F_o|$, for all reflections and $R_{free} = \Sigma||F_o| - |F_c||/\Sigma|F_o|$, calculated based on the 5% of data excluded from refinement.

Glu270, producing an ester bond with the newly formed C−O bond length at 1.3 Å. The attendant thiirane ring opening results in the thiolate of the covalently linked inhibitor as the fourth ligand to the tetrahedral catalytic zinc ion, along with three ligands from the protein (His69, His 196, and Glu72), as stipulated by design paradigms. The position of the thiolate as a zinc ligand was previously occupied by a water molecule in the apo enzyme. Furthermore, the inhibitor establishes a salt bridge to Arg145 via its carboxylate group and hydrogen bonds to Tyr248 and Asn144 side chains. Its isobutyl side chain is ensconced in the center of the hydrophobic pocket of the active site. The hydrophobic pocket is defined by approximately 9 Å of separation from top to bottom (Thr268 to Ala250) and left to right (Ser253 to Ile247), with Ile243 and Ile255 pair at the deep end. The conserved, CPA-type specificity-determinant residue Ile255 lies 6.3 Å from the inhibitor, the longest separation when comparing the bound and unbound CPA structures (hproCPA4, 5.2 Å; hproCPA2, 5.7 Å; hCPA4 (peptide-bound), 5.6 Å; bCPA (inhibitor-bound), 5.8 Å). A schematic representation of the binding of inhibitor **11** is shown in Figure 2C. An analysis of the contact areas between the catalytic domain and the pro-domain is given in Figure S2.

Inhibitor-induced conformational changes have been studied, both in the active and zymogenic forms of MCPs.[20,28] As compared to "unliganded" pro-CPA crystal structures,[27,29] the most striking difference is that of Tyr248, which undergoes an inhibitor-induced conformational change, whereupon the ring switches its position 120° between the surface-located "open" conformation to the "close" conformation, where the phenolic hydroxyl of the amino acid establishes a hydrogen bond to the carboxylate of the inhibitor (2.7 Å).[20,30] As indicated earlier, the terminal carboxylate of the inhibitor makes additional hydrogen bonds to Arg145 and Asn144 (Nδ1). All these contacts are

DOI: 10.1021/acsmedchemlett.7b00346
ACS Med. Chem. Lett. 2017, 8, 1122−1127

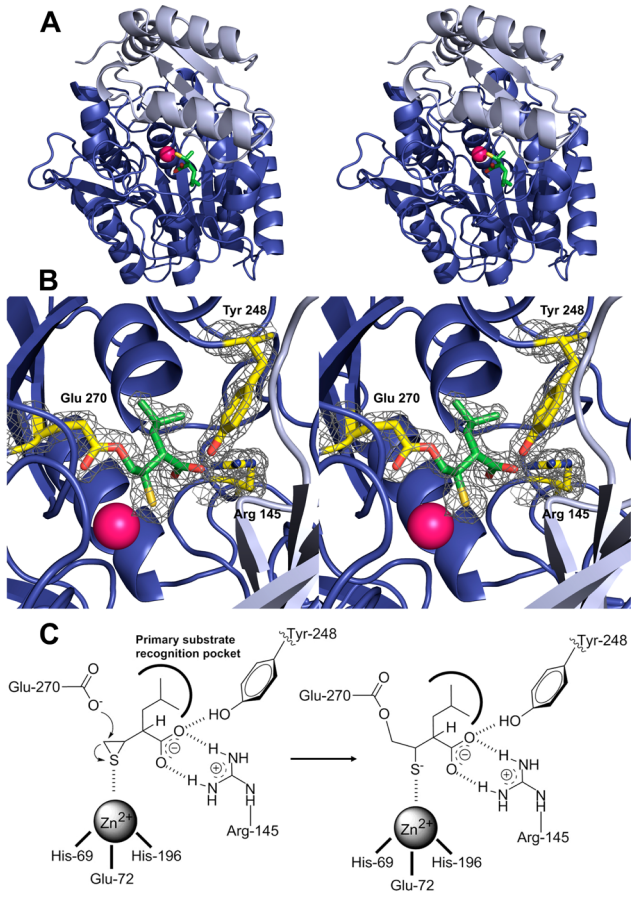

Figure 2. (A) Stereoimage of human proCPA1 in complex with compound **11**. The backbone of the pro and the catalytic domains are shown in gray and blue, respectively. The inhibitor is shown in capped sticks. (B) 2_{Fobs}-F_{calc} electron-density map showing the hCPA1 active site covalently bound inhibitor **11**, calculated by deleting the Glu270 side chain and inhibitor coordinates, is contoured at 1.5σ level. The inhibitor and residues important for binding (labeled) are shown in capped sticks (green and yellow, respectively). The catalytic zinc ion is in magenta, while the sulfur is in yellow. Oxygen and nitrogen are colored red and blue, respectively. A continuous electron density is clearly observed along the bond linking Glu270 side chain and the inhibitor. (C) Schematic representation of the binding of inhibitor **11**.

important for the proper sequestration of the inhibitor within the active site. Geometric details of inhibitor−enzyme interactions are listed in Table S3.

As with the benzyl moiety in phenylalanine in a typical peptide substrate of CPA, the isobutyl group of the inhibitor makes close contacts with the residues that configure the hydrophobic pocket, namely, Ala250 (3.4 Å), Ile243 (3.7 Å), and Thr268 (3.8 Å). In the present structure, we can observe substantial conformational changes, compared to other CPA1 (the activated enzyme) structures with bound ligands.[31,32] Thr268 reorients its side chain to contact the inhibitor via its hydroxyl group, changing its most common rotamer conformation of the χ_1 dihedral angle from *gauche* to *anti*.[33] These rearrangements would reflect the ability of the enzyme to adapt the size and the shape of the hydrophobic pocket to the characteristics of the ligand molecule, despite it being different from that of the natural peptide substrate. We add here that the basis for lack of inhibition of the related CPB by compound **11** and its analogues is likely the presence of an acidic residue at the distal end of the hydrophobic pocket. This acidic residue interacts with a positively charge amino acid from the substrate, which penetrates the recognition pocket; hence, inhibitor **11** discriminates against the CPB.

The crystal structure of thiirane-bound hpro-CPA1 has been used for molecular modeling of the spectroscopically nonsilent inhibitor **22** as an example of compounds that may act as tracking or imaging probes. As can be seen in Figure 3, such

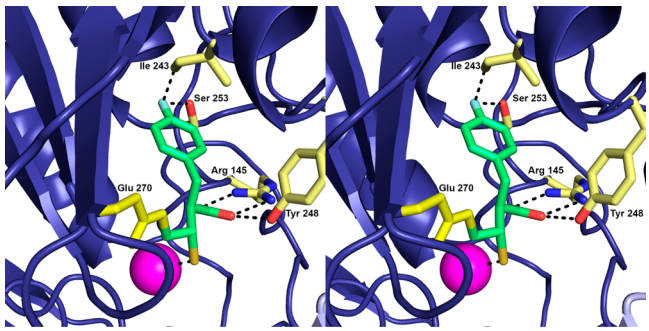

Figure 3. Molecular modeling of the hCPA1−fluorine inhibitor complex structure. The inhibitor and residues important for binding are shown in capped sticks, in green and yellow, respectively. The catalytic zinc ion is in magenta, the sulfur is in yellow, and the fluorine is in light blue. Oxygens and nitrogens are in red and blue, respectively. The model has been constructed with PyMOL using PDB file 5OM9.

fluorinated inhibitor molecule would fit into the active site of hCPA1 with the fluoro-substituted phenyl ring anchoring in the hydrophobic S1′ pocket of the enzyme. No steric clashes are observed in the model, consistent with the favorable kinetic results that we measured.

We have documented that our thiirane- and oxirane-based library of aliphatic and substituted aromatic compounds were able to inhibit a well-studied zinc protease, CPA. We can conclude that the inhibitory activity of these compounds was CPA-specific, as opposed to CPB, which was not inhibited. Per design paradigms, the time-dependence of kinetics and the high-resolution X-ray structure of **11** in complex to human CPA1 zymogen support it as a mechanism-based inactivator. The structure presented in this work represents the first human carboxypeptidase zymogen in complex with a mechanism-based inhibitor. Although all inhibitors were prepared as racemic mixtures, the crystal structure of the enzyme inhibited by compound **11** reveals that only the 2*R*,3*R* configuration, the one that corresponds to the D-amino-acid series,[25] could fit to the electron-density map. This indicates that the enzyme is enantioselective in its interaction with the inhibitor, coincident with what was reported for an oxirane inhibitor.[25]

Interestingly, the small-molecule thiirane is able to negotiate the physical barrier of the pro-domain in human pro-CPA1. This illustrates the feasibility of employing such a technology for tracing the fate and the location of the target enzymes using imaging technology, as exemplified by the fluorinated derivative (Figure 3). The fact that these compounds are agents that are converted to the inhibitory species only within the active site of the target enzyme holds the promise for new tools in biomedical research.

DOI: 10.1021/acsmedchemlett.7b00346
ACS Med. Chem. Lett. 2017, 8, 1122−1127

■ ASSOCIATED CONTENT

Supporting Information

The Supporting Information is available free of charge on the ACS Publications website at DOI: 10.1021/acsmedchemlett.7b00346.

Experimental details, synthesis, kinetic studies, and X-ray crystallographic statistics (PDF)

Accession Codes

The crystallographic coordinates are deposited in the Protein Data Bank (PDB code 5OM9).

■ AUTHOR INFORMATION

Corresponding Authors

*Tel: +34 935 812 154. E-mail: irantzu.pallares@uab.cat.
*Tel: +1 574 631-2933. E-mail: mobashery@nd.edu.

ORCID

Shahriar Mobashery: 0000-0002-7695-7883

Present Address

§(S.A.T.) Instituto de Química Rosario−IQUIR (CONICET), Facultad de Ciencias Bioquímicas y Farmacéuticas, Universidad Nacional de Rosario, Suipacha 531, Rosario S2002LRK, Argentina.

Author Contributions

The first two authors contributed equally to this work. S.A.T. designed and synthesized compound, C.G. purified proteins and performed the enzymatic analysis and the crystallization trials, D.F. made the preliminary enzymatic analysis and refined the X-ray structure, G.C. purified proteins and performed enzymatic analysis, P.G. and D.R. worked on complex crystallization and determined the 3D structure, I.P. calculated kinetic data, determined the X-ray structure, and prepared the figures, and S.A.T., C.G., S.M., I.P., J.V., and F.X.A. wrote the paper with input from coauthors.

Funding

Support from MINECO, grants BIO2013-44973R and BIO2016-78057R is gratefully acknowledged.

Notes

The authors declare no competing financial interest.

■ ACKNOWLEDGMENTS

The authors wish to thank Prof. Maya Chávez for helpful discussions.

■ REFERENCES

(1) Perez-Silva, J. G.; Espanol, Y.; Velasco, G.; Quesada, V. The Degradome database: expanding roles of mammalian proteases in life and disease. *Nucleic Acids Res.* **2016**, *44* (D1), D351−D355.

(2) Tanco, S.; Tort, O.; Demol, H.; Aviles, F. X.; Gevaert, K.; Van Damme, P.; Lorenzo, J. C-terminomics Screen for Natural Substrates of Cytosolic Carboxypeptidase 1 Reveals Processing of Acidic Protein C termini. *Mol. Cell. Proteomics* **2015**, *14* (1), 177−190.

(3) Sapio, M. R.; Fricker, L. D. Carboxypeptidases in disease: Insights from peptidomic studies. *Proteomics: Clin. Appl.* **2014**, *8* (5−6), 327−337.

(4) Rawlings, N. D.; Barrett, A. J.; Bateman, A. MEROPS: the database of proteolytic enzymes, their substrates and inhibitors. *Nucleic Acids Res.* **2012**, *40* (D1), D343−D350.

(5) de la Vega, M. R.; Sevilla, R. G.; Hermoso, A.; Lorenzo, J.; Tanco, S.; Diez, A.; Fricker, L. D.; Bautista, J. M.; Aviles, F. X. Nna1-like proteins are active metallocarboxypeptidases of a new and diverse M14 subfamily. *FASEB J.* **2007**, *21* (3), 851−865.

(6) Zhao, X. J.; Lu, C. P.; Chu, W. W.; Zhang, Y. X.; Zhang, B.; Zeng, Q.; Wang, R. F.; Li, Z.; Lv, B. L.; Liu, J. B. microRNA-214 Governs Lung Cancer Growth and Metastasis by Targeting Carboxypeptidase-D. *DNA Cell Biol.* **2016**, *35* (11), 715−721.

(7) Huang, S. F.; Wu, H. D. I.; Chen, Y. T.; Murthy, S. R. K.; Chiu, Y. T.; Chang, Y.; Chang, I. C.; Yang, X. Y.; Loh, Y. P. Carboxypeptidase E is a prediction marker for tumor recurrence in early-stage hepatocellular carcinoma. *Tumor Biol.* **2016**, *37* (7), 9745−9753.

(8) Denis, C. J.; Lambeir, A. M. The potential of carboxypeptidase M as a therapeutic target in cancer. *Expert Opin. Ther. Targets* **2013**, *17* (3), 265−279.

(9) Lyons, P. J.; Sapio, M. R.; Fricker, L. D. Zebrafish Cytosolic Carboxypeptidases 1 and 5 Are Essential for Embryonic Development. *J. Biol. Chem.* **2013**, *288* (42), 30454−30462.

(10) Vovchuk, I. L.; Petrov, S. A. Role of carboxypeptidases in carcinogenesis. *Biomed. Khim.* **2008**, *54* (2), 167−178.

(11) Fan, S. L.; Li, X.; Li, L. M.; Wang, L. G.; Du, Z. Z.; Yang, Y.; Zhao, J. S.; Li, Y. Silencing of carboxypeptidase E inhibits cell proliferation, tumorigenicity, and metastasis of osteosarcoma cells. *OncoTargets Ther.* **2016**, *9*, 2795−2803.

(12) Fernandez, D.; Pallares, I.; Covaleda, G.; Aviles, F. X.; Vendrell, J. Metallocarboxypeptidases and their Inhibitors: Recent Developments in Biomedically Relevant Protein and Organic Ligands. *Curr. Med. Chem.* **2013**, *20* (12), 1595−1608.

(13) Kim, D. H.; Mobashery, S. Mechanism-based inhibition of zinc proteases. *Curr. Med. Chem.* **2001**, *8* (8), 959−965.

(14) Forbes, C.; Shi, Q. C.; Fisher, J. F.; Lee, M.; Hesek, D.; Llarrull, L. I.; Toth, M.; Gossing, M.; Fridman, R.; Mobashery, S. Active Site Ring-Opening of a Thiirane Moiety and Picomolar Inhibition of Gelatinases. *Chem. Biol. Drug Des.* **2009**, *74* (6), 527−534.

(15) Ruiz-Cabello, J.; Barnett, B. P.; Bottomley, P. A.; Bulte, J. W. M. Fluorine (F-19) MRS and MRI in biomedicine. *NMR Biomed.* **2011**, *24* (2), 114−129.

(16) Kruger, A.; Arlt, M. J. E.; Gerg, M.; Kopitz, C.; Bernardo, M. M.; Chang, M.; Mobashery, S.; Fridman, R. Antimetastatic activity of a novel mechanism-based gelatinase inhibitor. *Cancer Res.* **2005**, *65* (9), 3523−3526.

(17) Kim, D. H. Chemistry-based design of inhibitors for carboxypeptidase A. *Curr. Top. Med. Chem.* **2004**, *4* (12), 1217−1226.

(18) Brown, S.; Bernardo, M. M.; Li, Z. H.; Kotra, L. P.; Tanaka, Y.; Fridman, R.; Mobashery, S. Potent and selective mechanism-based inhibition of gelatinases. *J. Am. Chem. Soc.* **2000**, *122* (28), 6799−6800.

(19) Testero, S. A.; Lee, M.; Staran, R. T.; Espahbodi, M.; Llarrull, L. I.; Toth, M.; Mobashery, S.; Chang, M. Sulfonate-Containing Thiiranes as Selective Gelatinase Inhibitors. *ACS Med. Chem. Lett.* **2011**, *2* (2), 177−181.

(20) Fernandez, D.; Testero, S.; Vendrell, J.; Aviles, F. X.; Mobashery, S. The X-Ray Structure of Carboxypeptidase A Inhibited by a Thiirane Mechanism-Based Inhibitor. *Chem. Biol. Drug Des.* **2010**, *75* (1), 29−34.

(21) Kim, D. H.; Chung, S. J. Inactivition of Carboxypeptidase-A by 2-Benzyl-3,4-Epithiobutanoic acid. *Bioorg. Med. Chem. Lett.* **1995**, *5* (15), 1667−1672.

(22) Vendrell, J.; Cuchillo, C. M.; Aviles, F. X. The tryptic activation pathway of monomeric procarboxypeptidase A. *J. Biol. Chem.* **1990**, *265* (12), 6949−6953.

(23) Rajendra, G.; Miller, M. J. Intramolecular electrophilic additions to olefins in organic syntheses. Stereoselective synthesis of 3,4-substituted.beta.-lactams by bromine-induced oxidative cyclization of O-acyl.beta.,.gamma.-unsaturated hydroxamic acid derivatives. *J. Org. Chem.* **1987**, *52* (20), 4471−4477.

(24) Kim, Y. M.; Kim, D. H. Convenient preparation of all four possible stereoisomers of 2-benzyl-3,4-epoxybutanoic acid, pseudo-mechanism-based inactivator for carboxypeptidase a via alpha-chymotrypsin-catalyzed hydrolysis. *Bull. Korean Chem. Soc.* **1996**, *17* (10), 967−969.

(25) Ryu, S. E.; Choi, H. J.; Kim, D. H. Stereochemistry in inactivation of carboxypeptidase A. Structural analysis of the

DOI: 10.1021/acsmedchemlett.7b00346
ACS Med. Chem. Lett. 2017, 8, 1122−1127

inactivated carboxypeptidase A by an enantiomeric pair of 2-benzyl-3,4-epoxybutanoic acids. *J. Am. Chem. Soc.* **1997**, *119* (1), 38−41.
(26) Kitz, R.; Wilson, I. B. Ester of Methanesulfonic Acid as Irreversible Inhibitors of Acetyl Cholinesterase. *J. Biol. Chem.* **1962**, *237* (10), 3245−3249.
(27) Garcia-Saez, I.; Reverter, D.; Vendrell, J.; Aviles, F. X.; Coll, M. The three-dimensional structure of human procarboxypeptidase A2. Deciphering the basis of the inhibition, activation and intrinsic activity of the zymogen. *EMBO J.* **1997**, *16* (23), 6906−6913.
(28) Fernandez, D.; Boix, E.; Pallares, I.; Aviles, F. X.; Vendrell, J. Analysis of a New Crystal Form of Procarboxypeptidase B: Further Insights into the Catalytic Mechanism. *Biopolymers* **2010**, *93* (2), 178−185.
(29) Guasch, A.; Coll, M.; Aviles, F. X.; Huber, R. Three-Dimensional structure of Porcine Pancreatic Procarboxypeptidase-A. A Comparison of the A-Zymogen and B-Zymogen and their Determinants for Inhibition and Activation. *J. Mol. Biol.* **1992**, *224* (1), 141−157.
(30) Cho, J. H.; Kim, D. H.; Chung, S. J.; Ha, N. C.; Oh, B. H.; Choi, K. Y. Insight into the stereochemistry in the inhibition of carboxypeptidase A with N-(hydroxyaminocarbonyl) phenylalanine: Binding modes of an enantiomeric pair of the inhibitor to carboxypeptidase A. *Bioorg. Med. Chem.* **2002**, *10* (6), 2015−2022.
(31) Mangani, S.; Carloni, P.; Orioli, P. Crystal Structure of the Complex Between Carboxypeptidase A and the Biproduct Analog Inhibitor L-benzylsuccinate at 2.0 Angstroms Resolution. *J. Mol. Biol.* **1992**, *223* (2), 573−578.
(32) Fernández, D.; Boix, E.; Pallarès, I.; Avilés, F. X.; Vendrell, J. Structural and Functional Analysis of the Complex between Citrate and the Zinc Peptidase Carboxypeptidase A. *Enzyme Res.* **2011**, *2011*, 128676.
(33) Pallares, I.; Fernandez, D.; Comellas-Bigler, M.; Fernandez-Recio, J.; Ventura, S.; Aviles, F. X.; Bode, W.; Vendrell, J. Direct interaction between a human digestive protease and the mucoadhesive poly(acrylic acid). *Acta Crystallogr., Sect. D: Biol. Crystallogr.* **2008**, *64*, 784−791.

DOI: 10.1021/acsmedchemlett.7b00346
ACS Med. Chem. Lett. 2017, 8, 1122−1127